

Supporting information

***In-situ* Raman spectroscopic insight into charge delocalization- improved electrical conductivity in metal–cyanide frameworks**

Zhixuan Lu,^{ab} Yajun Huang,^a Liting Shao,^a Maofeng Cao,^a Shu Hu,^a Chuan Liu,^a Xiang Wang^a and Bin Ren^{*ac}

^a*State Key Laboratory of Physical Chemistry of Solid Surfaces, Collaborative Innovation Center of Chemistry for Energy Materials (i-ChEM), Department of Chemistry, College of Chemistry and Chemical Engineering, Xiamen University, Xiamen 361005, China*

^b*Institute of Luminescent Materials and Information Displays, College of Materials Science and Engineering, Huaqiao University, Xiamen 361021, China.*

^c*Innovation Laboratory for Sciences and Technologies of Energy Materials of Fujian Province (IKKEM), Xiamen 361005, China*

Corresponding Author

*Corresponding author. E-mail: bren@xmu.edu.cn

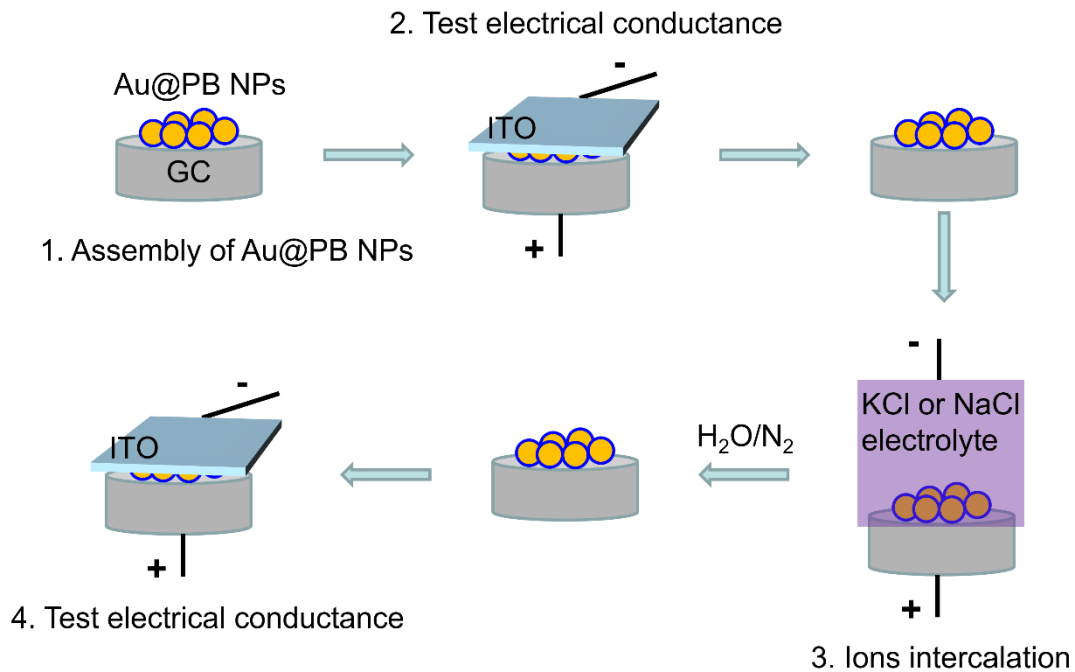


Figure S1. Amperometric *i*-*V* measurement for the electrical conductance of Au@PB NPs and Au@PB NPs intercalated with alkali metal ions. The conductive surface of the ITO is facing downward.

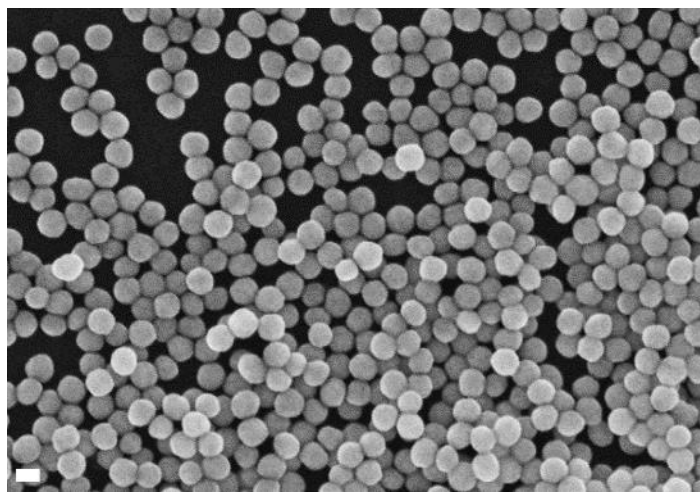


Figure S2. SEM image of Au NPs. Scale bars: 50 nm.

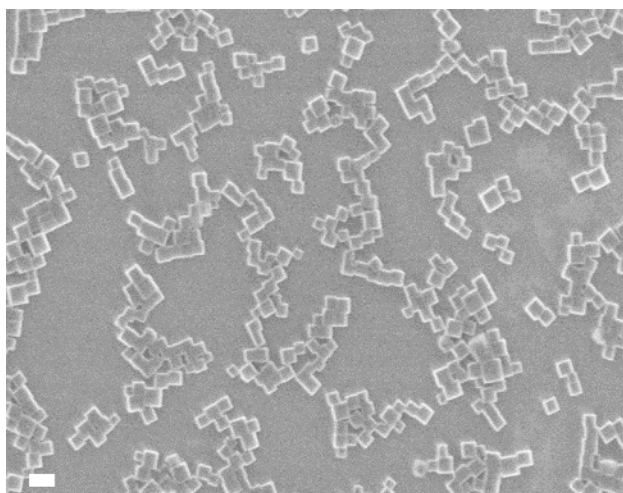


Figure S3. SEM image of PB NPs. Scale bars: 50 nm.

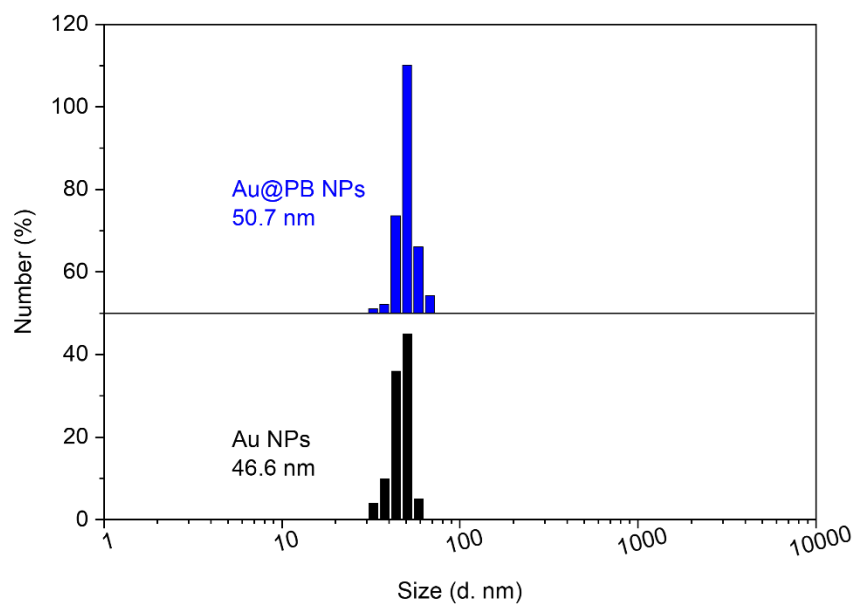


Figure S4. Dynamic light scattering data of the Au NPs (black) and Au@PB NPs with a 2 nm thick PB shell (blue).

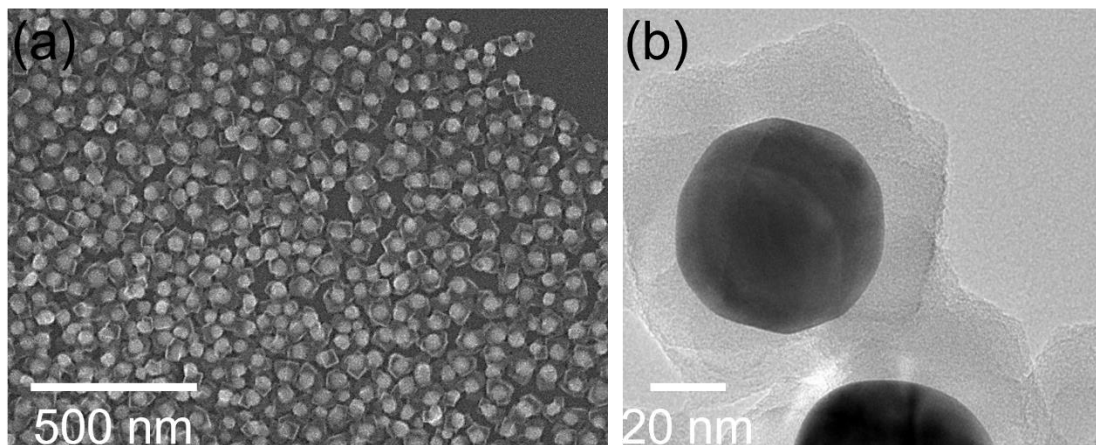


Figure S5. SEM (a) and TEM (b) images of the Au@PB NPs with a 20 nm thick PB shell.

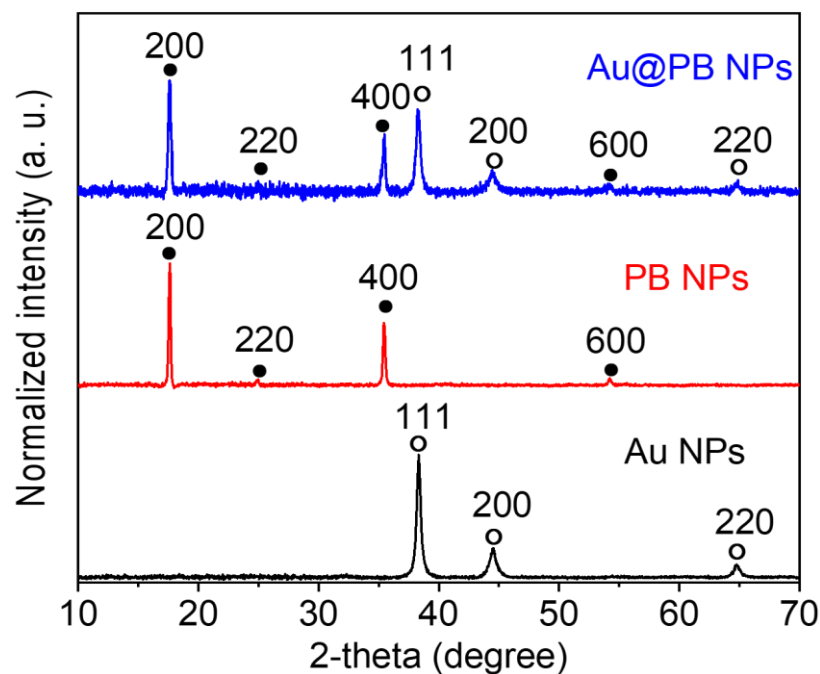


Figure S6. Powder X-ray diffraction (XRD) patterns of Au NPs (black), PB NPs (red), and Au@PB NPs with a 20 nm thick PB shell (blue). Two series of peaks are assigned to the Au core (JCPDS card no. 89-3697, marked with hollow circle) and the PB shell (JCPDS card no. 1-239, marked with solid circle).

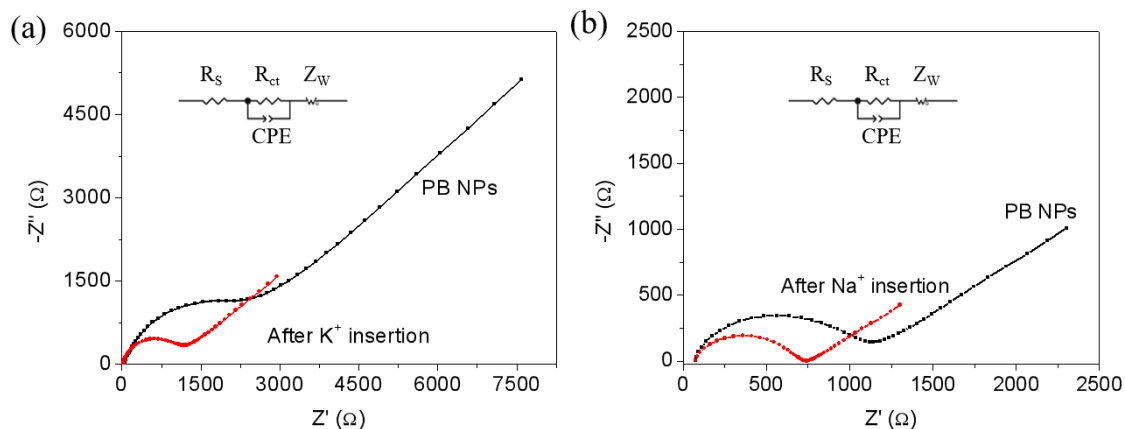


Figure S7. Typical Nyquist plots for before and after K (a) or Na (b) ions insertion PB NPs modified on GC electrode with aqueous solution of 1.0 M KCl or NaCl. Inset: equivalent circuit used in the fitting. R_s , series resistance; R_{ct} , charge transfer resistance; CPE, constant phase element; Z_W , Warburg impedance.

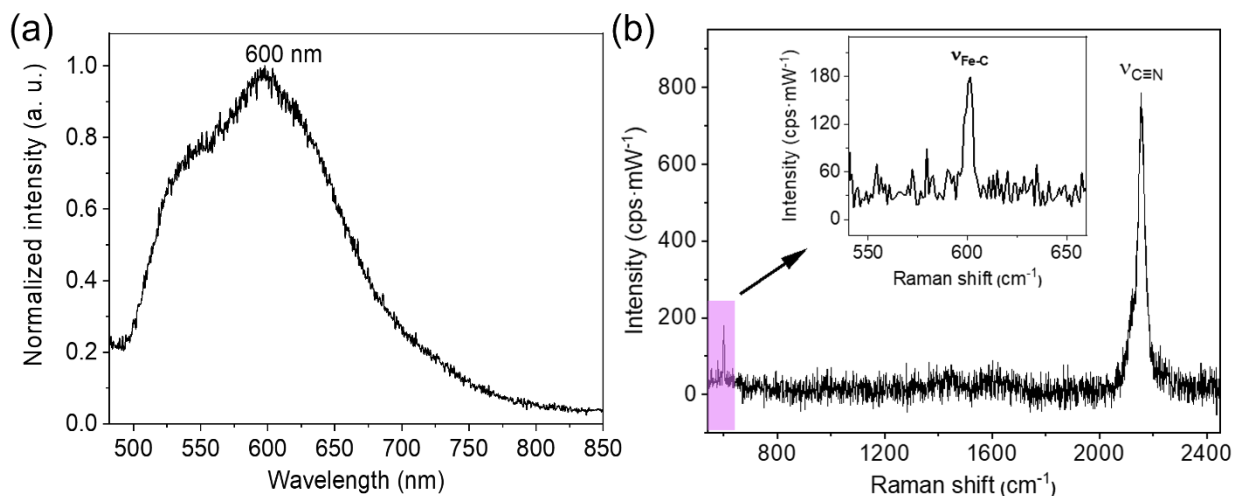


Figure S8. (a) The reflective absorption spectrum of Au@PB NPs deposited on glassy carbon electrode. (b) SERS spectrum of Au@PB NPs dispersed on a glassy carbon electrode substrate. The inset shows the Fe-C peak. The Raman spectrum was collected with an exposure time of 10 s and a laser power of 0.36 mW at 633 nm wavelength.

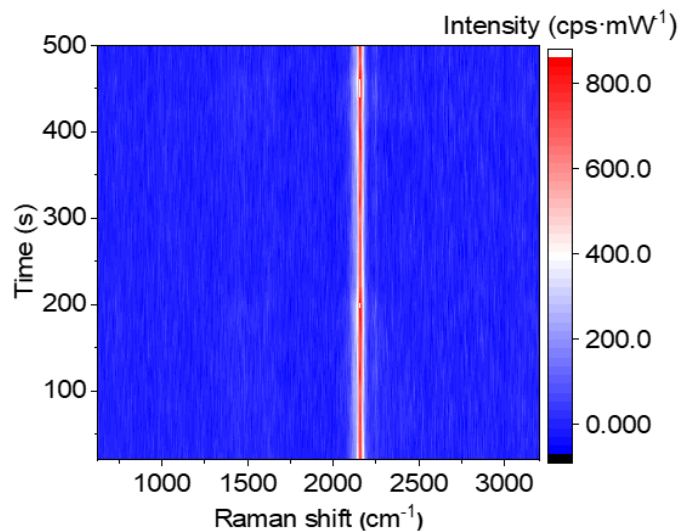


Figure S9. The time-dependent SERS spectra of Au@PB NPs dispersed on a glassy carbon electrode substrate. The Raman spectrum was collected with an exposure time of 10 s and a laser power of 0.36 mW at 633 nm wavelength.

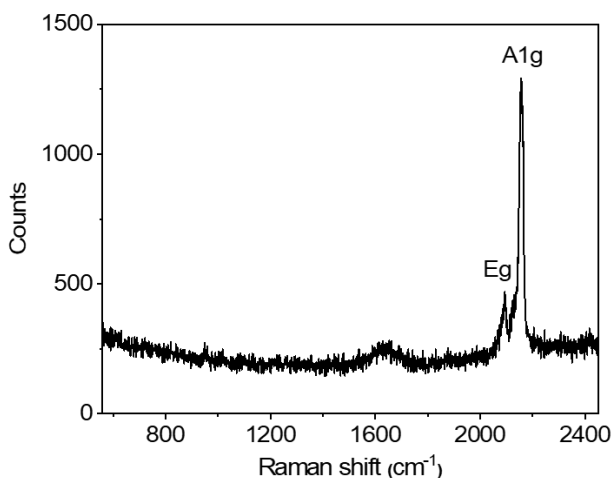


Figure S10. Normal Raman spectrum of PB NPs dispersed on a glassy carbon electrode substrate. The Raman spectrum was collected with an exposure time of 60 s and three times of accumulation and a laser power of 8.00 mW at 633 nm wavelength.

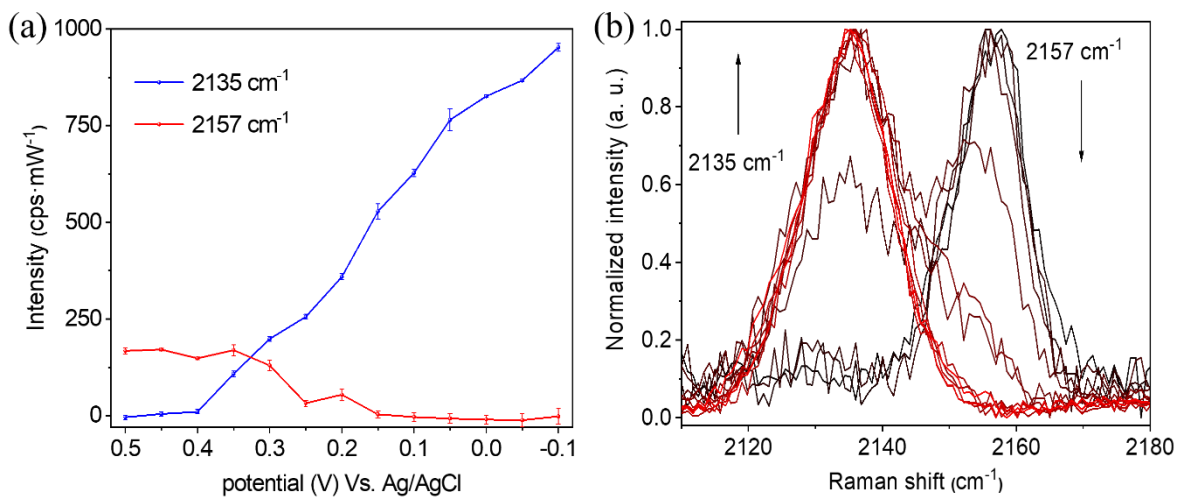


Figure S11. (a) The potential-dependent intensity of CN vibrations at 2157 cm⁻¹ (red) and 2135 cm⁻¹ (blue) and (b) normalized Raman spectra in the region of CN vibrations obtained during the insertion of K ions in PB for Au@PB NPs.

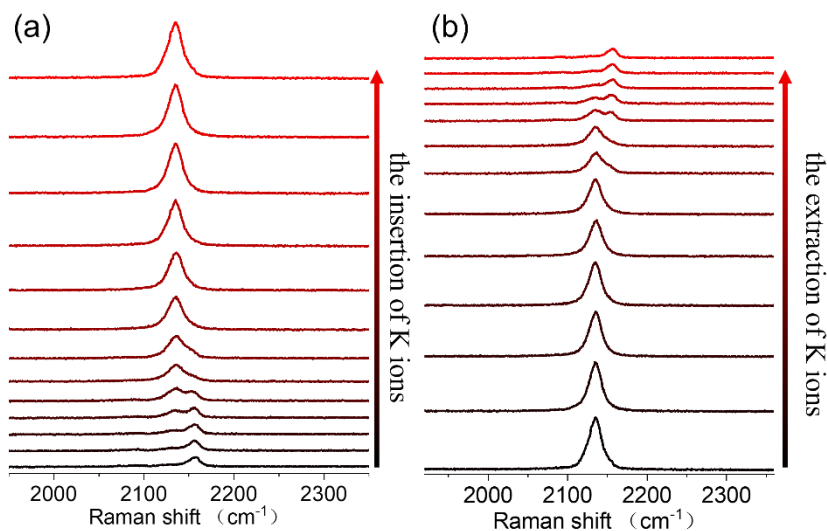


Figure S12. SERS spectra obtained during the insertion (a) and the extraction (b) of K ions in Au@PB NPs with a 20 nm thick PB shell.

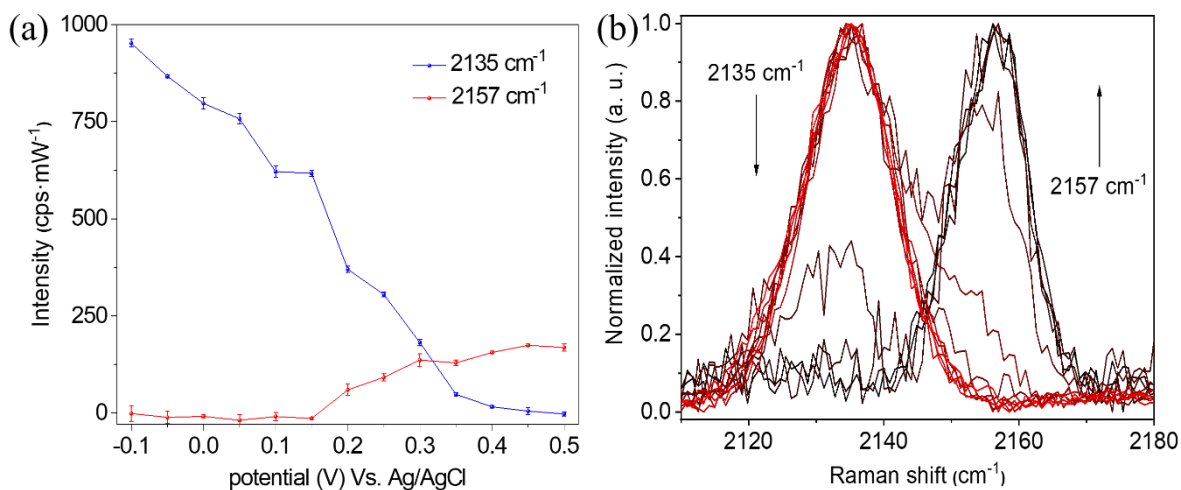


Figure S13. (a) The potential-dependent intensity of CN vibrations at 2157 cm⁻¹ (red) and 2135 cm⁻¹ (blue) and (b) normalized Raman spectra of CN vibrations during the extraction of K ions in PB for Au@PB NPs.

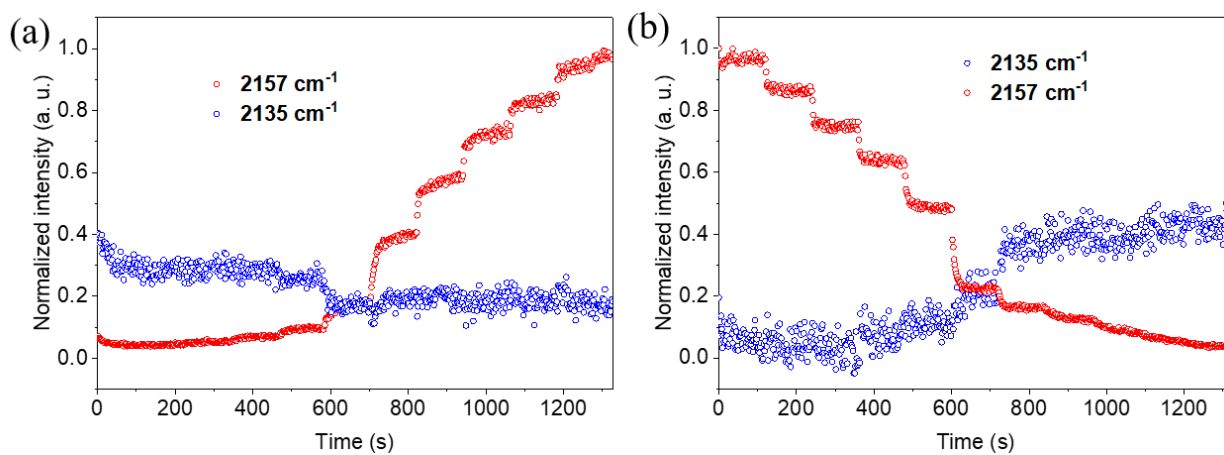


Figure S14. The time-dependent intensity of CN vibrations at 2157 cm⁻¹ (red) and 2135 cm⁻¹ (blue) obtained when step potentials were applied from -0.10 to 0.50 V (a) or from 0.50 to -0.10 V (b) with 0.10 V step interval.

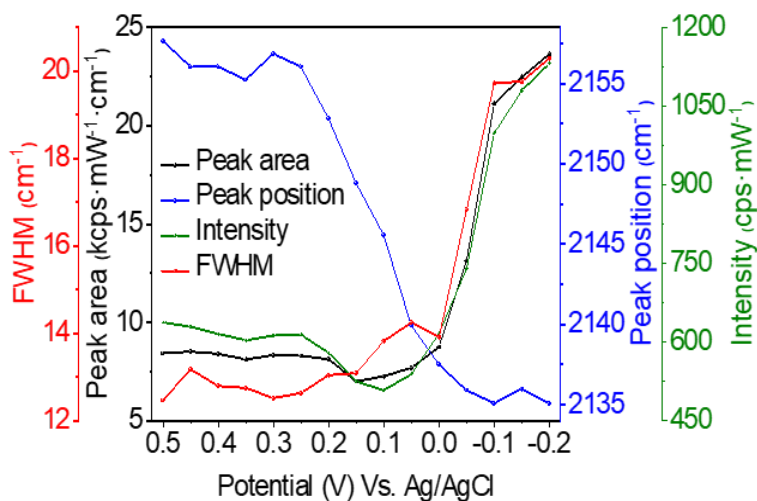


Figure S15. The potential-dependent position (blue), intensity (green), area (black) and FWHM (red) of the SERS peak of CN vibration during the insertion of Na ions in PB for Au@PB NPs.

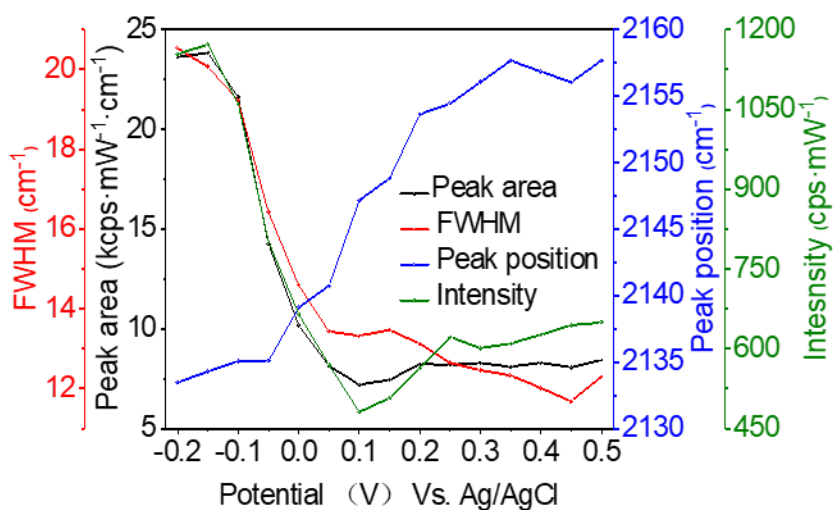


Figure S16. The potential-dependent position (blue), intensity (green), area (black) and FWHM (red) of the SERS peak of CN vibration during the extraction (d) of Na ions in PB for Au@PB NPs.

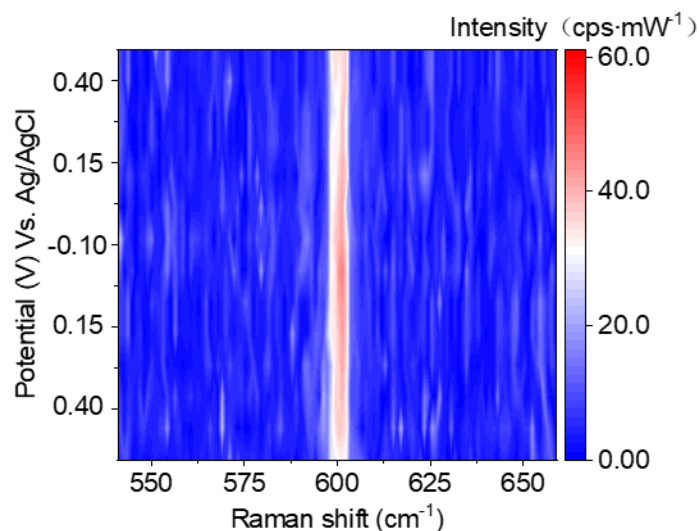


Figure S17. The EC-SERS spectra of Au@PB NPs are color-coded intensity map of CN bond at precise control potential from 0.50 V to - 0.10 V for K ions, respectively. SERS spectra were collected with an exposure time of 10 s at a laser power of 0.36 mW with the 633 nm laser.

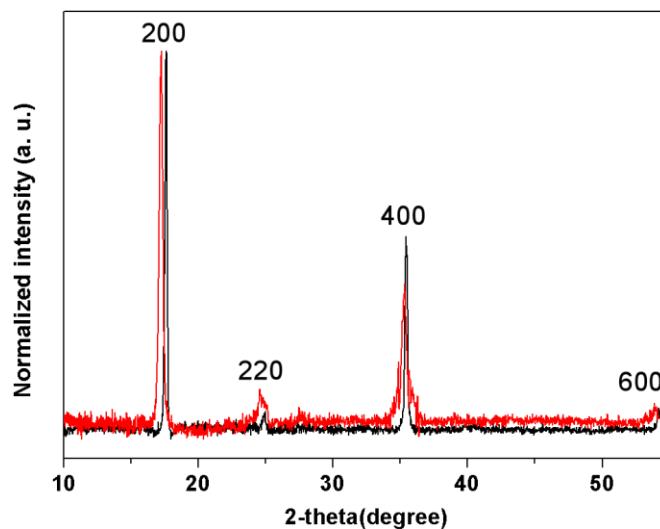


Figure S18. XRD patterns of before (black) and after (red) Na ions insertion into PB NPs. The diffraction peaks shift to smaller angles and the splitting of 220 peak indicate the lattice expansion, a characteristic of a solid the rhombohedral phase of PB.

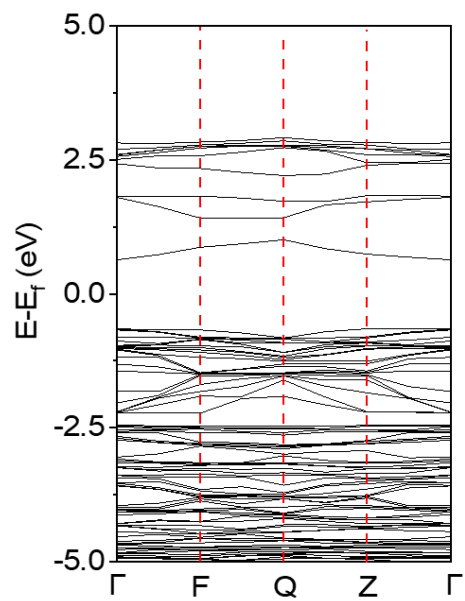


Figure S19. Calculated electronic band structure and density of states of PB.

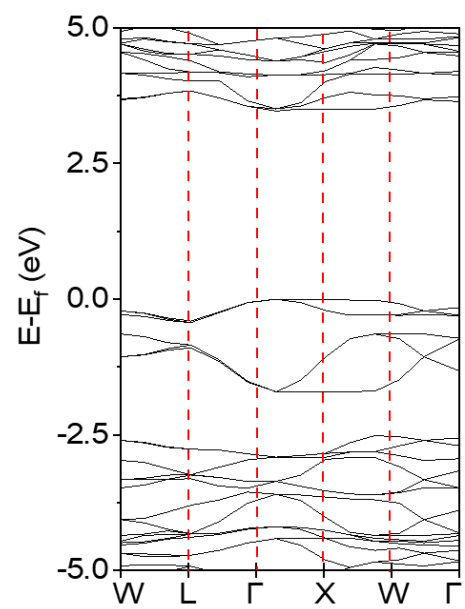


Figure S20. Calculated electronic band structure and density of states of K ions-inserted PB.